Manufacturing High Strength Aluminum Matrix Composites by Friction Stir Processing: An Innovative Approach

Nelson Netto[a], Lv Zhao[a,c,*], Jeroen Soete[b], Grzegorz Pyka[a], and Aude Simar[a]

[a] *Institute of Mechanics, Materials and Civil Engineering, UCLouvain, Louvain-la-Neuve, Belgium*
[b] *Department of Materials Engineering, KU Leuven, Leuven, Belgium*
[c] *Department of Mechanics, Huazhong University of Science and Technology, Wuhan, China*

** Correspondence: lv.zhao@uclouvain.be*

Abstract

Shape Memory Alloys (SMA), e.g., NiTi (nitinol), are good candidates of reinforcement agents for the improvement of mechanical properties of aluminum alloys. Friction Stir Processing (FSP) has been shown to be an appropriate manufacturing process for particulate Aluminum Matrix Composites (AMCs), due to the mitigation of critical intermetallic formation between particles and matrix. However, AMCs processed by FSP with the matrix material made of high strength alloys, in particular 7xxx series, have systematically shown severe defects, such as clusters and cavities that result from poor material flow. Herein, we present an innovative strategy to manufacture Al7075/NiTi composites via FSP avoiding this unacceptable particle clustering. The strategy involves the addition of 7xxx series Al powder in a groove or multi-holes to be stirred together with the NiTi particles, leading to dissociation of the latter. The X-ray computed tomography acquisitions allow for 3D quantitative assessment of the size and spatial distribution of the embedded reinforcements. It is revealed that the groove filling method results in a more homogenous distribution compared to the multi-holes filling method. Moreover, the distribution is found to be dependent on the particle size, as a higher volume fraction of large particles is observed at the upper part of the FSP stir zone. These new AMCs, with a good Al-NiTi interface, present a potential to tailor the composite mechanical properties by exploiting the shape memory effect of the NiTi reinforcements.

Keywords: Metal matrix composites, friction stir processing, shape memory alloys, microstructure defects, homogeneous distribution

1. Introduction

Embedding particulate reinforcements in aluminum matrices to form Aluminum Matrix Composites (AMCs) is an attractive, alternative and innovative process to enhance the mechanical properties of aluminum alloys. In the previous studies of Heinz et al. (2000) and Williams and Starke (2003), the authors have shown that high strength aluminum alloys, especially Al7075, are widely used in the aerospace industry due to their high strength-to-density ratio. Sharma et al. (2015) asserted that it is promising to introduce reinforcement particles into the aluminum matrix and to pursue superior mechanical properties, such as tensile strength.

Buehler et al. (1963) showed that Shape Memory Alloys (SMA), also known as smart materials, have the unique property of being able to recover their original shape throughout heating, the so called Shape Memory Effect (SME). Otsuka and Ren (2005) revealed that SME occurs as a result of phase change from the low temperature martensite to the high temperature austenite. Besides the direct use of SMAs for engineering applications, Porter et al. (2001) demonstrated that SMA particles could be used as reinforcements to further improve the mechanical properties of light metals. In that study, composite materials (Al1090/NiTi) exhibited higher yield and ultimate tensile strength but lower elongation compared with the base material. Recently, Zhao et al. (2019) demonstrated that inserting NiTi particles into the Al 1050 matrix and triggering the SME could introduce local internal stresses in the aluminum matrix. The stress fields around the NiTi particles fostered crack deviation and resulted in higher fracture toughness compared to the Al1050/NiTi composite without SME activation. Moreover, Cai et al. (2005) and Huang (2002) showed that SMA particles could also enhance the functional properties, such as damping capacity, with respect to the base material.

Regarding the integration of SMAs in metal matrices, Thorat et al. (2009) showed that it was not desirable to manufacture Metal Matrix Composites (MMCs) using common cast and Powder Metallurgy (PM) processes, due to severe interfacial reaction and interfacial diffusion occurring between the SMAs and the matrix alloys under high temperature. The same conclusion was found in the review provided by Ni and Ma (2014). Dixit et al. (2007) stated that the formation of intermetallics was detrimental to the interface bond strength and intermetallics would serve as key sites for damage initiation, leading to an early failure. Thorat et al. (2009) indicated that the presence of Al in the NiTi could also affect the phase transformation behavior and degrade the SME due to the variation in the composition of SMAs. Moreover, Nestler et al. (2011) pointed out that clustering of reinforcement particles was another critical issue in aluminum matrix composites manufactured via powder metallurgy, in addition to intermetallics. A homogeneous distribution of particles in the matrix is however of paramount importance for the manufacturing of AMCs in order to reach good mechanical properties, whatever the reinforcement agents. Indeed, Deng and Chawla (2006) reported through finite element simulations that higher degree of particle clustering could lead to earlier failure due to strain localization within the particle clusters.

Friction Stir Processing (FSP), a technique derived from friction stir welding (Mishra and Mahoney, 2001; Mishra et al., 1999), is a thermo-mechanical process to locally modify the microstructure. Mishra et al. (2003) used FSP to manufacture surface composites by adding reinforcements inside a groove or multi-holes in the workpiece prior to the processing. Ni et al. (2014) demonstrated that FSP prevails over powder metallurgy in the metal matrix composites manufacturing due to the fact that interfacial reaction barely takes place in solid state, and as such, intermetallic formation can be significantly reduced.

The dispersion of reinforcement particles in a metal matrix by FSP is achieved by intense material flow. FSP has been successfully employed in manufacturing low strength AMCs by Dixit et al. (2007) and intermediate strength AMCs by Ni et al. (2014), resulting in a clean interface and reasonably homogeneous particle distribution in both materials. However, it should be noted that FSP may lead to two types of defects in the manufactured MMCs, i.e., particle clusters and cavities. These defects are usually the consequence of insufficient heat input which results in poor material flow during FSP, as claimed by Kim et al. (2006). The particle clusters and pre-existing cavities can lead to stress concentrations and foster premature failure in the composites. By fine-tuning the process parameters and applying multiple passes, the aforementioned defects can be eliminated or largely reduced in most cases. However, when manufacturing AMCs based on 7xxx series Al alloys by FSP, severe particle clustering invariably arises, whatever the nature of reinforcements and the process parameters.

Rana et al. (2016) manufactured Al7075/B4C composites by FSP with the reinforcements pre-embedded in a groove (groove filling method). Large clusters and cavities were generated, and particle accumulation was observed on the advancing side. According to the authors, it would be impossible to move the particles from the advancing to the retreating side with insufficient material flow. Though the authors tried to improve the flow by changing the traverse speed, no significant improvement was obtained. In the same research group, Rana and Badheka (2018) later used multi-holes to pre-embed the reinforcements (multi-holes filling method) while keeping the same base material and reinforcement particles. The authors explored several combinations of rotational and traverse speeds in order to improve the particle distribution. Although they reported that a lower rotational speed could reduce the size of the particle clusters, cavities and cluster defects always remained in the microstructure.

Gangil et al. (2018) manufactured Al7050/TiB_2 composites with the groove filling method by FSP. The reinforcement particles were around 1 μm in diameter, which are much smaller than the B_4C particles (10 μm) used by Rana et al. (2016). The authors conducted a single FSP pass and listed cluster sizes and locations within the cross section. According to the authors, clusters in the center, on the advancing side, and on the retreating side differ in size due to differences in material flow and stirring action. Nevertheless, the authors did not propose a remedy to eliminate these undesirable defects.

The particle clustering is formed due to limited material flow that inherently results from the very high mechanical strength of the 7xxx Al matrix. The limited material flow also has the tendency to produce a sintering effect, i.e., a number of reinforcement particles join together to form much larger particles under heat and pressure. These aforementioned drawbacks lead to the fact that homogeneous particle distribution in FSP manufactured 7xxx Al based AMCs cannot be achieved, regardless of the reinforcement size and the process parameters. This manufacturing related issue, however, needs to be tackled to enable the tailoring of mechanical properties of high strength Al alloys via reinforcements.

In the present study, we propose a new strategy to manufacture Al7075/NiTi composites by FSP, which avoids particle sintering and significantly reduces particle clustering. Instead of using only the reinforcement particles, a powder of the base material (Al7075) was first mixed into the NiTi particles, which were then embedded together into the matrix by FSP. The aluminum powder has the potential to create barriers between the NiTi particles and thus reduces particle agglomeration. As a result, the NiTi particles can be homogeneously dispersed in the Al7075 matrix, without sintered particles or particle clustering, while keeping the advantage of FSP in terms of impeding intermetallic formation. It is worth mentioning that the mixing strategy allows easily tailoring the reinforcement content and investigating its influence on the mechanical properties.

2. Experimental procedure

Commercial plates of Al7075-T6 (Zn – 5.85 wt.%, Mg – 2.51 wt.%, Cu – 1.65 wt.%, Fe – 0.1 wt.%, Si – 0.04 wt.%, Mn – 0.03 wt.%, Cr – 0.2 wt.%, Al – bal) with dimensions of 200×80×6 mm were used in this study. Based on literature, both multi-holes and groove were used to pre-integrate the reinforcement particles. For the multi-holes case, a series of 20 holes with 3 mm in diameter and 4.5 mm in depth were machined in the center and perpendicularly to the plate surface, as schematically shown in Fig. 1. The distance between the hole centers was 6 mm. For the groove case, a groove of 2.5 mm in width and 4 mm in depth was machined in the center of the plate. A cover plate of 0.7 mm was used to avoid particle loss during the process. Two powders were used in this study, i.e., atomized equiatomic NiTi particles with mean diameter of 79 μm and Al7075 powder with mean diameter of 50 μm. In order to prepare a homogeneously mixed powder composed of 50 vol% of NiTi powder and 50 vol% of Al powder, the two aforementioned powders were placed in a turbula mixer for 24h. In addition, a reference composite with only NiTi powder was manufactured in order to investigate the effect of the new mixing strategy.

FSP was conducted on a commercial friction stir welding machine manufactured by Tra-C industrie. Optimum process parameters were selected based on the surface finish smoothness and the absence of cavities. After several trials, the process parameters were set to a rotational speed of 400 rpm and a traverse speed of 100 mm min^{-1}. A conical FSP tool was used. The tool was composed of a shoulder 20 mm in diameter and a right-hand threaded conical pin with major diameter equal to 8 mm and minor diameter equal to 6 mm and length equal to 5.2 mm. The FSP tool was tilted 1° opposite to the processing direction and the plunge depth was controlled to be 5.5 mm for each pass. Furthermore, the tool was carefully aligned with the center of the holes or grooves in order to fully process the powder region. To investigate the effect of multiple passes on the particle size and distribution, 4, 6 and 8 passes were conducted, with a 100% overlap and the same forward direction. The manufactured composites were then brought to the hardest T6 state via a solution treatment at 470ºC for 1h, followed by aging at 120ºC for 24h as suggested by Lyman (1964).

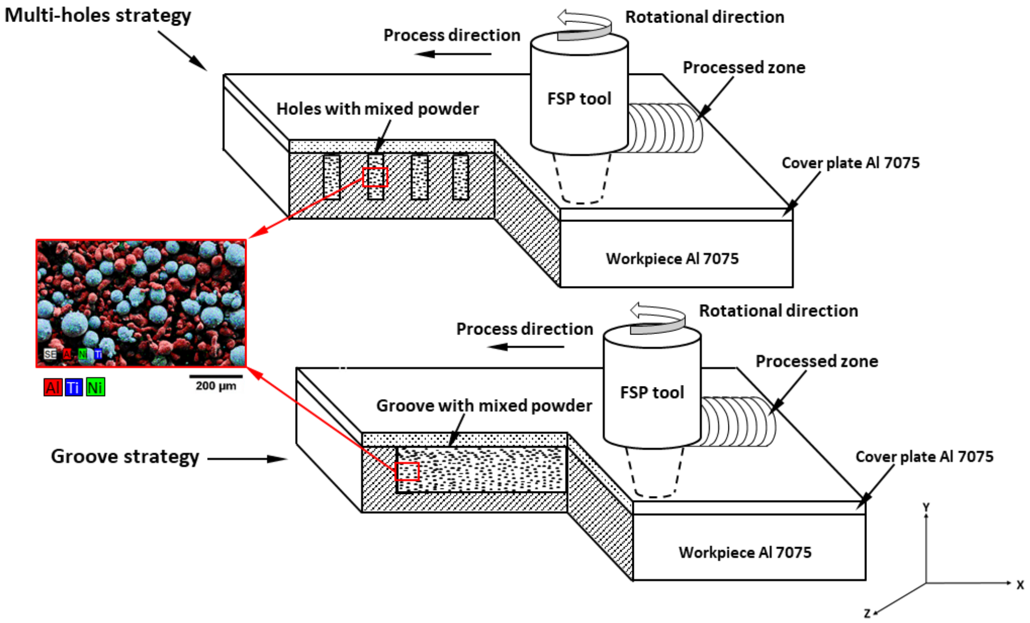

Fig. 1. Schematic of the manufacturing process of composites by FSP with a partial cut showing the multi-holes (top) and groove (bottom) filled with mixed powder (the EDX map shows blue particles as NiTi powder and red particles as Al7075 powder).

The samples for microstructural examinations were sectioned perpendicular and parallel to the FSP direction and were prepared by a standard polishing procedure. The overview distribution of the NiTi particles in the Al matrix was assessed using a ZEISS FEGSEM Ultra 55 Scanning Electron Microscope (SEM). The size and distribution of the embedded NiTi particles in the Al matrix were evaluated with high resolution X-ray Computed Tomography (HRXCT), using a Phoenix Nanotom S 180 kV system (from General Electric). The HRXCT samples (6×3×3 mm) were extracted by electrical discharge machining from the center of the FSP stir zone. Scanning was performed at a voxel size of 2 µm. The analysis of the HRXCT datasets was performed with Avizo 9.5 software (ThermoFisher Scientific).

Internal pores in the NiTi particles have been introduced during the powder manufacturing process, but they do not influence the potential crack propagation blocking mechanism in the composites. However, these internal pores could affect the particle separation process when treating the HRXCT dataset. A morphological operation was applied to remove the internal particle cavities, which are mainly present in large particles. Next, a watershed based approach was applied to separate detected particles. In a first step, the particle volume was defined by an automatic global thresholding approach using the Otsu (1979) segmentation method. This process starts with computing the Chamfer Distance maps and the contrast regional maxima (H-Maxima) of the reconstructed image. In this way the watershed separation lines were generated and subtracted from the binary image of particles to complete the separation process. As a next step, particles that touch the borders of the HRXCT dataset were eliminated.

For each filling condition and number of FSP passes, two tensile specimens were machined parallel to the FSP direction by Electrical Discharge Machining (EDM) following the E8-M ASTM standard for sub-size specimen, with the gauge being completely within the stir zone. The specimens were extracted 2 mm below the top surface of the plates, and then mechanically polished to have a smooth surface, with a cross-sectional thickness of 1.5 mm. Tensile tests were performed using a Zwick tensile machine instrumented with an extensometer attached to the specimen throughout the test. The extensometer gauge length was 22 mm and the tests were carried out at a constant loading rate of 1 mm/min.

3. Results and discussions

3.1. 2D microstructure characterization

The cross section of the manufactured composite with only the NiTi powder is shown in Fig. 2a. It can be noticed that sintered NiTi particles, which can reach more than 1 mm in size, have been formed at both the retreating (Fig. 2b) and advancing (Fig. 2c) sides after 6 passes. As a result, a very low quantity of NiTi particles is present in the center of the FSP stir zone. This defect type is also present after 4 and 8 passes, indicating that the number of FSP passes cannot improve the particle distribution.

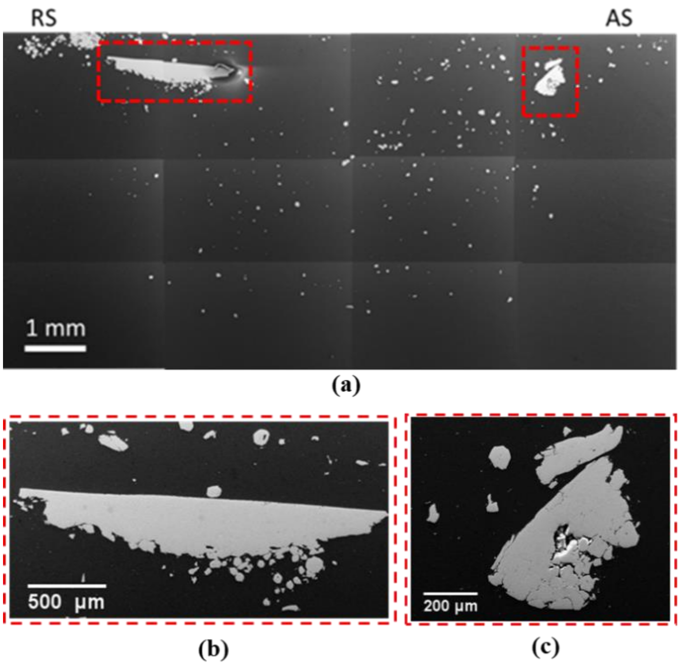

Fig. 2. Cross section of the composite manufactured (6 passes) with only NiTi powder embedded in multi-holes observed by SEM (a), sintered particles on RS (b) and AS (c), respectively. RS = retreating side, AS = advancing side.

The formation of clustering and sintering of NiTi particles during FSP is the outcome of insufficient material flow due to the high strength of the Al7075 matrix. It should be mentioned that NiTi particles of similar size have been homogeneously integrated in both 1xxx and 6xxx series of Al matrices, as reported respectively by Dixit et al. (2007) and Ni et al. (2014). However, all previous studies on FSPed composites with 7xxx series Al matrices showed cluster defects, whatever reinforcement nature and size, as stated in the introduction section. The result presented in Fig. 2 confirms this general trend reported in literature. As the material flow is poor, the reinforcement particles cannot be dispersed outside the pin region, they thus interact repeatedly with each other via inter-particle friction and form sintered particles. In literature, Zeng et al. (2018) used an artificially thickened oxide layer during the friction stir welding of Al2014-T6 to track the material flow, with the oxide layer acting as tracer. The authors reported the formation of an “S” line in the microstructure, which represents the flow of the oxide layer. The line is shifted to the retreating side implying that the flow is therefore more intense at the RS. This information is relevant for AMC research, since it allows to understand how the reinforcement particles are distributed into the aluminum matrix, and in particular why clustering occurs at some preferred locations. In the present Al7075/NiTi composites, given the poor material flow and the reinforcement interactions, the NiTi particles tend to agglomerate and sinter more severely at the retreating side, as shown in Fig. 2a.

Furthermore, fragments of NiTi particles can be observed in this reference composite. According to Huang et al. (2018) the fragmentation of particles is a result of plastic deformation and stirring action of the FSP tool during the process. However, it is important to keep the NiTi particles in particulate shape in order to obtain good bonding with the Al matrix and avoid stress concentrations when subjecting the composites to external loading. Large fragments of irregular shape are more likely to be damage initiation sites, thus degrading the mechanical properties of the composites. Although the NiTi particles were successfully embedded in the lower strength matrix of the Al 6061 series, small fragments and irregular shape particles were still observed, as reported in Ni et al. (2014).

Fig. 3a shows the cross section of the composites manufactured (8 passes) with the mixed powder embedded using the **multi-holes filling method**. In contrast to using only the NiTi powder, the strategy of mixing Al powder with NiTi powder effectively avoids severe particle clustering and sintering (compare Fig. 3a with Fig. 2a). In addition, Fig. 3b shows that the NiTi particles retain a spherical shape. Moreover, no micron scale intermetallic layer can be seen at the interface. Though severe clustering and sintering are no longer present in the composite, the particle distribution is still not perfectly homogeneous, as reflected by the lower particle density towards the retreating side (see Fig. 3a).

Regarding the composites manufactured (8 passes) with the mixed powder embedded using the **groove filling method**, the cross-sectional microstructure does not present any evident clustering or sintering defects either, as shown in Fig. 4. The particle density is higher compared to the multi-holes strategy, since more NiTi particles have been pre-integrated in the continuous groove. The particle distribution using the groove strategy seems more homogeneous compared to the multi-holes strategy, especially in the region close to the retreating side. A more detailed 3D characterization with the HRXCT datasets will be presented in the following sub-section.

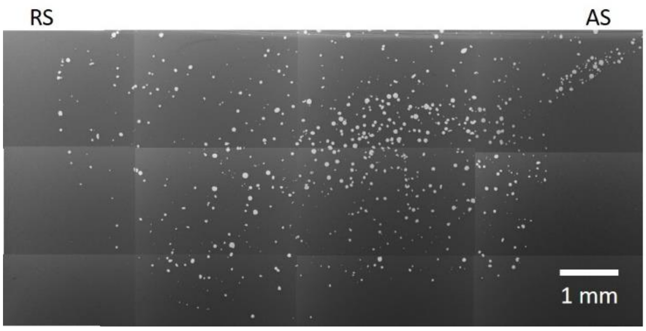

(a)

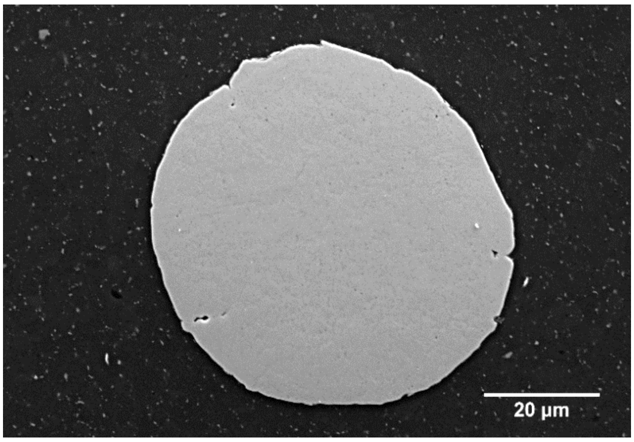

(b)

Fig. 3. Cross section of the composite manufactured (8 passes) with the mixed powder embedded in the multi-holes observed by SEM (a), zoom of one representative NiTi particle retaining its spherical shape after 8 passes (b).

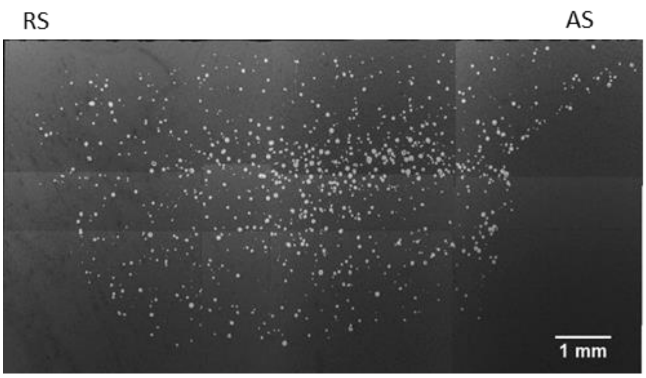

Fig. 4. Cross section of the composite manufactured (8 passes) with the mixed powder using the groove filling method, showing uniformly distributed NiTi particles (observation with SEM).

To the authors' knowledge, this is the first time a composite has been made with the matrix of 7xxx Al alloys by FSP, presenting reasonably homogeneous particle distribution while keeping clean interfaces between the reinforcements and the matrix. This powder mixture approach allows overcoming the issues of manufacturing high strength Al matrix based composites by FSP and should be applicable to other types of reinforcements.

As the multi-holes filling method involves discontinuous pre-integration of reinforcement particles, SEM side view images of the composites are provided in Fig. 5 to illustrate where the HRXCT samples have been extracted from the composites manufactured with the multi-holes filling method. Fig. 5a presents the case after 4 FSP passes, where repeated agglomerations of particles at the upper part can be seen. These agglomerations correspond to the initial hole locations, as indicated by the white dotted box. For the tomography analysis, the sample has been extracted between holes, as outlined by the red dotted box. Fig. 5b presents the side view after 8 FSP passes, one can barely determine where the holes were initially located due to the absence of agglomeration. The same observation has been conducted for the groove filling method, at first sight, the particle distribution seems homogeneous in the FSP direction even after 4 FSP passes since the mixed powder was continuously pre-embedded. However, a particle agglomeration at the upper part of the FSP stir zone is still observed and will be further discussed based on the HRXCT datasets.

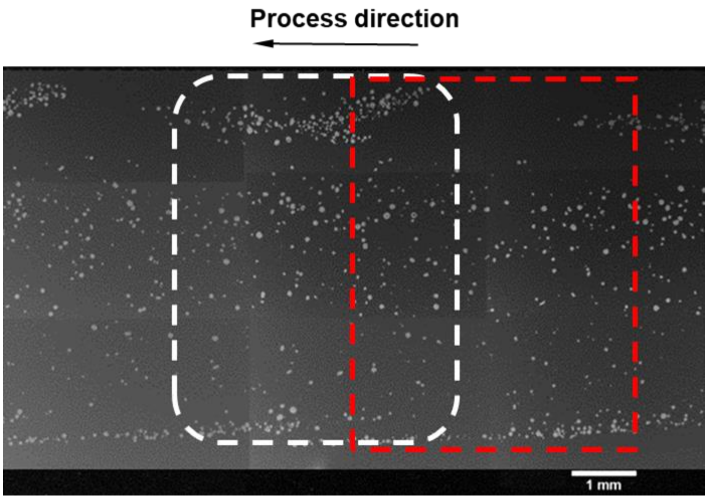

(a)

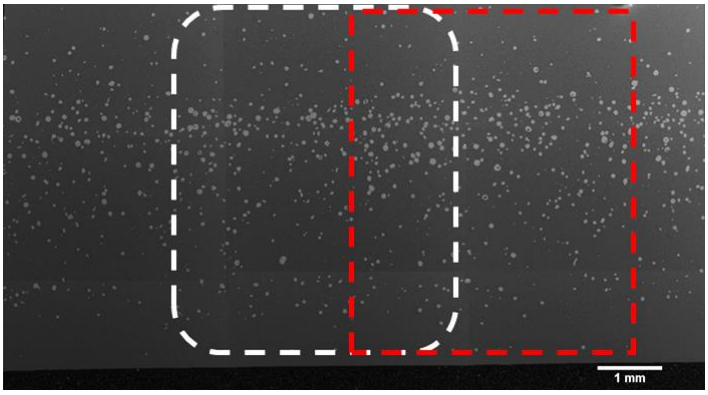

(b)

Fig. 5. Scanning electron microscopy (SEM) side view images of the composites manufactured with 4 passes (a) and 8 passes (b) using the mixed powder and the multi-holes filling method. The red and white dotted box show the location where the samples for tomography were extracted and the initial hole position, respectively.

3.2. 3D rendering of particle distribution by high resolution 3D X-ray tomography

In order to investigate the effect of multiple passes and compare the two pre-integration methods, i.e., the multi-holes and groove strategies, the volume fraction and spatial distribution of the NiTi particles in the composites have been statistically analyzed with HRXCT.

Fig. 6 shows the 3D side view renderings of the center of the FSP stir zone for 4 and 8 passes with both the multi-holes and groove filling methods. The x-axis represents the FSP direction (Note that the samples are not color-coded and the difference in color is to show different samples). The groove filling method grants a much higher volume fraction of NiTi particles, which is consistent with the 2D cross section views (see Figs. 3a and 4). For the multi-holes method, as presented in Fig. 6a and 6b, it is found that the NiTi particle distribution remains strongly inhomogeneous after 4 passes, with zones empty of NiTi particles (see top of Fig. 6a). The empty space corresponds to the interval between two adjacent holes at the extraction location of the HRXCT sample (see also Fig. 5a). After 8 passes, the NiTi particles are more homogenously distributed, as can be observed in Fig. 6b. An increase in number of FSP passes for the multi-holes filling method can thus significantly improve the distribution of NiTi reinforcements.

In the case of groove filling method, Fig. 6c shows that the particles are already well distributed into the center of the stir zone after only 4 passes, which is in contrast to the multi-holes filling method with the same number of passes. Fig. 6d presents the results after 8 FSP passes. No significant improvement can be observed in the spatial distribution compared to the 4 passes case, suggesting that the homogenization of particles could already be achieved with 4 passes.

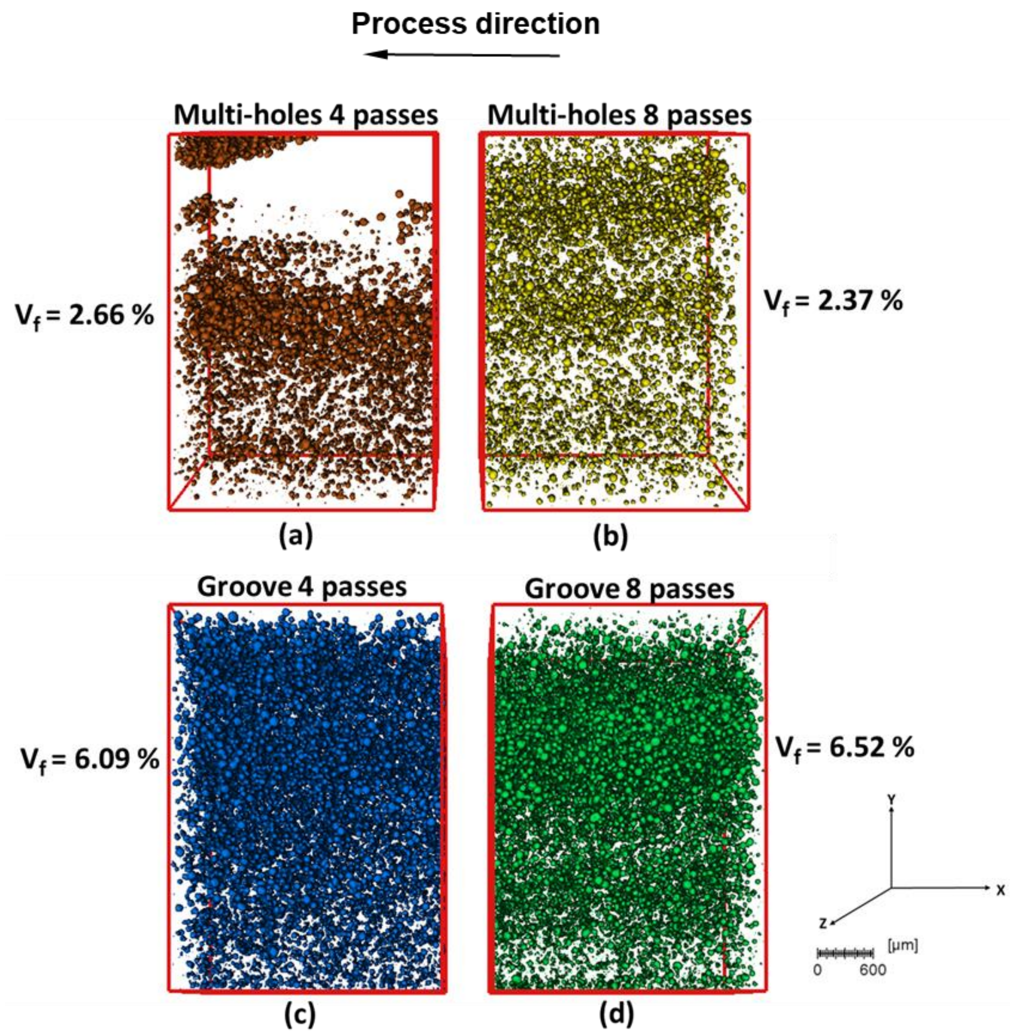

Fig. 6. 3D particle distribution in the HRXCT datasets, for the multi-holes filling method after 4 passes (a) and 8 passes (b), and for the groove filling method after 4 passes (c) and 8 passes (d). The coordinate system is identical to that of Fig. 1. The particle volume fraction (V_f) for each condition is also reported.

3.3. Quantitative assessment of particle distribution

To characterize the degree of homogeneity, the distribution of NiTi particles has been assessed with the nearest-neighbor distance (NN_D) distribution. Netto et al. (2018) and Tiryakioglu and Netto (2018) have characterized the distribution of secondary phase in aluminum alloys after multiple FSP passes. They showed that the nearest-neighbor distance distribution is an efficient way to quantify the homogeneity level of the microstructure. The NN_D is defined as the distance between centroids of a given particle and its closest neighbor. The NN_D distribution for all conditions has been fitted by hypothesizing that it follows a lognormal distribution, which is consistent with results reported in literature. The Anderson-Darling goodness-of-fit tests (Anderson and Darling, 1954) have been conducted to test this hypothesis. In all four cases, the hypothesis that the data follow the lognormal distribution is reasonable, as can be seen from the histogram and the corresponding lognormal fitting for the groove filling method after 8 passes (see Fig. 7a). The comparisons between the histograms and the fittings for the other cases are presented in Fig. S1 of the supplementary material. The probability density function for the lognormal distribution is written as:

$$f(NND) = \frac{1}{NND\sigma\sqrt{2\pi}} exp\left[\frac{-(ln(NND)-\mu^2)}{2\sigma^2}\right] \tag{1}$$

where σ is the shape and μ is the scale parameter. The expectance, i.e., the mean of the lognormal distribution is calculated by:

$$\overline{NND} = e^{\mu+\frac{\sigma^2}{2}} \tag{2}$$

The parameters of the lognormal distribution have been estimated by using the maximum likelihood method. They are presented in Table 1. The probability density functions of NN_D for the multi-holes and groove methods are presented together in Fig. 7b. Though severe clusters are not present in any of the samples, increasing the number of passes, especially for the multi-holes condition, leads to varying particle distribution, i.e., the NN_D increases with more passes. Indeed, the mean NN_D distances, calculated using Eq. 2, are 87 μm and 100 μm after 4 and 8 passes, respectively, for the multi-holes filling method. Lower values of NN_D can be associated with inhomogeneous distribution, i.e., local particle concentration can reduce the distance between the closest neighbors. With more FSP passes, the NiTi particles move to previously unoccupied zones in the aluminum matrix, leading to a more homogenous distribution. This is in agreement with what has been observed in the HRXCT datasets (see Fig. 6).

For the groove condition, no significant difference can be observed between the NN_D distributions of 4 and 8 passes. The mean NN_D distances calculated by Eq. 2, are 79 μm and 77 μm after 4 and 8 passes, respectively. The mean distance is shorter than the case of multi-holes since more NiTi particles are integrated, as reflected by the much higher volume fraction of NiTi particles (see Fig. 6). Hence, for the groove condition, 4 passes are sufficient to achieve a homogeneous distribution of NiTi particles in the aluminum matrix.

Due to the inevitable difference in the volume fraction (V_f) between the groove and multi-holes conditions, as mentioned in the above paragraph, the homogeneity of the NiTi particle distribution for the two filling methods after 8 passes cannot be directly compared in terms of the mean NN_D values. In order to determine which filling strategy promotes a more homogeneous reinforcement distribution after a sufficient large number of FSP passes, an additional criterion is required.

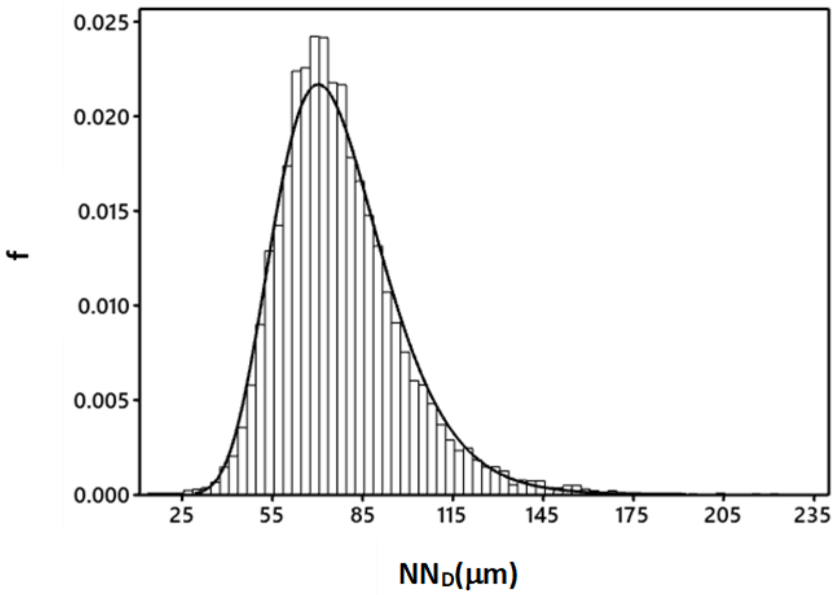

(a)

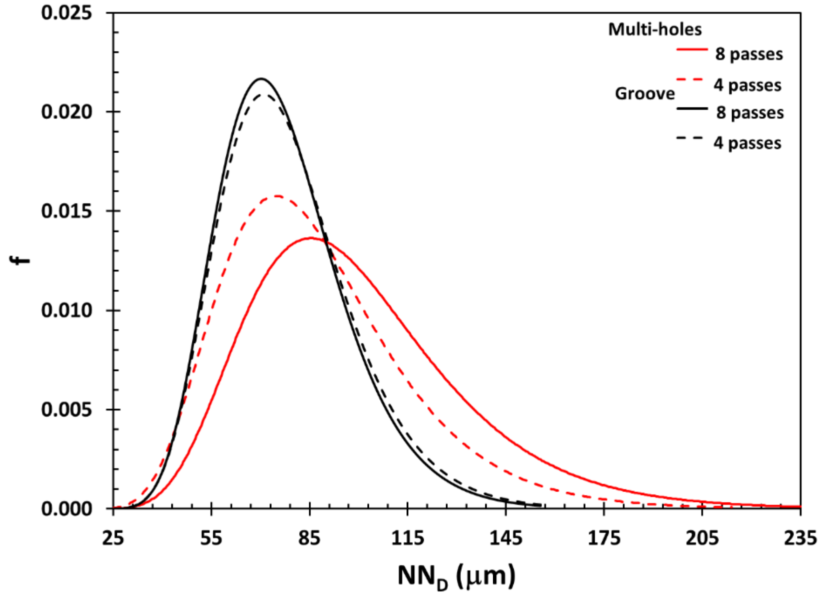

(b)

Fig. 7. Histogram and fitted lognormal distribution for the groove filling method after 8 passes (a), probability density functions of NN_D (following Eq. 1) after 4 and 8 passes for both the multi-holes and the groove filling methods (b).

Table 1. Estimated parameters of the lognormal distributions for NN_D for groove and multi-holes conditions after 4 and 8 passes.

	Groove		Multi-holes	
FSP passes	σ	μ	σ	μ
4	0.254	4.316	0.325	4.553
8	0.261	4.330	0.321	4.418

Yang et al. (2001) have demonstrated that the coefficient of variance of the nearest neighbor distance (COVd) is an effective parameter to characterize the homogeneity of reinforcement distribution. Moreover, the authors have shown that the COVd is not sensitive to the particle morphology or the volume fraction, which is suitable for the present work. COVd parameter can be calculated by:

$$COVd = \frac{\sigma_d}{\overline{NND}} \tag{3}$$

Where σ_d represents the variance in the mean NN_D, and for a lognormal distribution this is calculated by:

$$\sigma_d = \overline{NND}(e^{\sigma^2} - 1) \tag{4}$$

$\overline{NND}$ is defined in Eq. 2 and the values of σ have been provided in Table 1.

Deng and Chawla (2006) used the COVd parameter to characterize particle clustering for Al matrix composites reinforced with SiC particles. The authors reported that higher COVd was related to more severe particle clustering, and as this parameter decreased, a more homogenous microstructure was observed.

In the present work, for the composites manufactured with the groove condition after 4 and 8 FSP passes, the COVd value was 5.15 and 5.53, respectively. For the multi-holes condition with the same number of passes, the COVd value was 11.14 and 9.47 (4 and 8 FSP passes), i.e. significantly higher than that for the groove filling method. This indicates that the groove filling method prevails over the multi-holes one in terms of the homogeneity of particle integration by FSP.

3.4. Quantitative assessment of particle size

To characterize the effect of multiple passes on the particle size, the equivalent diameter (d_{eq}) was measured based on the HRXCT datasets. A bimodal distribution (number-weighted) has been observed in all the scanned samples, as presented in Fig. S2 of the supplementary material. This indicates that there are 2 particle size groups. The first group contains smaller particles, with a diameter range from 15 to 35 μm and a local mode of 25 μm. The second group contains larger particles, with a diameter range from 35 to 120 μm and a local mode of 56 μm. Similar to the NN_D, the d_{eq} of both size groups follows a lognormal distribution. The histograms and their lognormal fittings for all four samples (two filling strategies and two numbers of passes) are shown in Fig. S2. The estimated parameters of the lognormal distributions are presented in Table 2. As suggested by Weibull (1939), the probability density function (*f*) for a mixture of smaller and larger distributions is determined by:

$$f = f_1 * p + (1 - p) * f_2 \tag{5}$$

where *p* is the fraction of the first mode, the subscripts 1 and 2 refer to the smaller (first mode) and the larger (second mode) particle groups, respectively.

Table 2. Estimated parameters of the lognormal distributions of d_{eq} for the groove and multi-holes conditions after 4 and 8 passes.

	Groove			Multi-holes		
FSP passes	σ	μ	p	σ	μ	p
4 (smaller particles)	0.169	3.285	0.192	0.168	3.269	0.203
4 (larger particles)	0.246	4.089		0.251	4.093	
8 (smaller particles)	0.170	3.267	0.212	0.169	3.267	0.241
8 (larger particles)	0.255	4.108		0.257	4.101	

Fig. 8 shows the probability density functions for the multi-holes and groove conditions after 4 and 8 passes. Two observations are worth mentioned. First, increasing the number of FSP passes from 4 to 8 passes favors the formation of smaller particles for both the multi-holes and groove filling methods; second, the probability of the larger particle mode for the multi-holes strategy is lower compared to the groove strategy, and the probability of the smaller particle mode is higher accordingly. This indicates that large particles are more easily and frequently reduced in size when they are pre-integrated in multi-holes. This phenomenon could be explained by the fact that the multi-holes condition involves more NiTi-Al matrix interaction, in particular in regions between the drilled holes, while for the groove condition, the NiTi particles interact more with the Al particles which flow better than the bulk Al matrix. In this sense, the groove filling condition should be preferred in terms of impeding particle fragmentation.

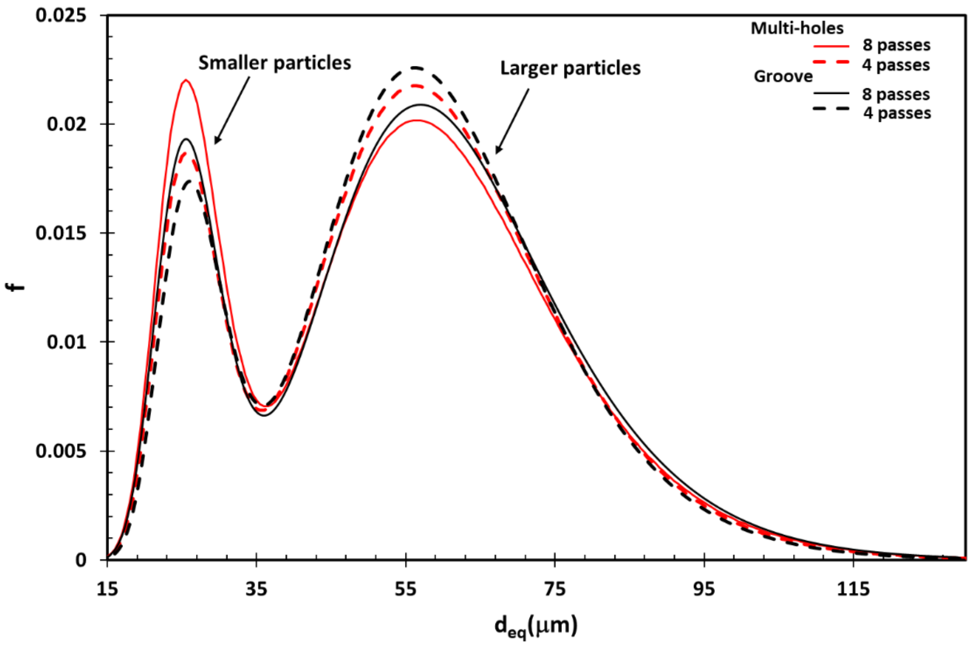

Fig. 8. Probability density functions of d_{eq} after 4 and 8 passes for both the multi-holes and groove filling methods.

As the NiTi particles present a large range of sizes, it is then interesting to investigate the particle distribution in function of the particle size. This investigation addresses the samples with the groove filling method for 4 and 8 FSP passes, which present very similar global distribution characteristics (Fig. 6c and d).

The spatial distributions of NiTi particles involving different d_{eq} ranges are presented in Fig. 9. The 3D rendering of the selected samples (the same as presented in Fig. 6c and d) have been divided into four size classes, i.e., 20-40 μm, 40-80 μm, 80-120 μm and larger than 120 μm, see Fig. 9. A very similar distribution is observed between 4 and 8 passes. For the smallest particle class (20-40 μm, Fig. 9a and e), the NiTi particle distribution appears highly homogeneous, without any visible particle clustering throughout the sample. In contrast, when the particle size increases (40-80 μm, Fig. 9b and f), a slight particle agglomeration site (in a band shape) is observed at the upper part of the sample, presenting a larger local particle density. Regarding the particle class of 80-120 μm (Fig. 9c and g), the concentration at the upper part of the sample is even more apparent, especially for the 8 FSP passes. Only few particles with d_{eq} > 120µm (Fig. 9d and h) have been detected, which is another indication that the powder mixture counteracts the formation of larger particles by sintering. It can therefore be concluded that the particle distribution in the Al matrix is more homogeneous for small NiTi particles. The inhomogeneous distribution for large particles sizes needs further investigation. It could be attributed to the surplus in material flow towards the bottom of the tool pin, as reported by Prado et al. (2003) .

This result is of paramount importance for the optimization of the manufacturing process of AMC, where the NiTi powder can be filtered into a desired particle range prior to FSP, and only ranges that favor homogeneous particle distributions can be used during the FSP treatment. Typically particles with d_{eq} > 80 µm are more difficult to transport. Combining with the mixing powder method, the reduction in the powder d_{eq} size can further enhance the homogenization in the aluminum matrix. More research is needed in the future to evaluate its effect on the mechanical properties.

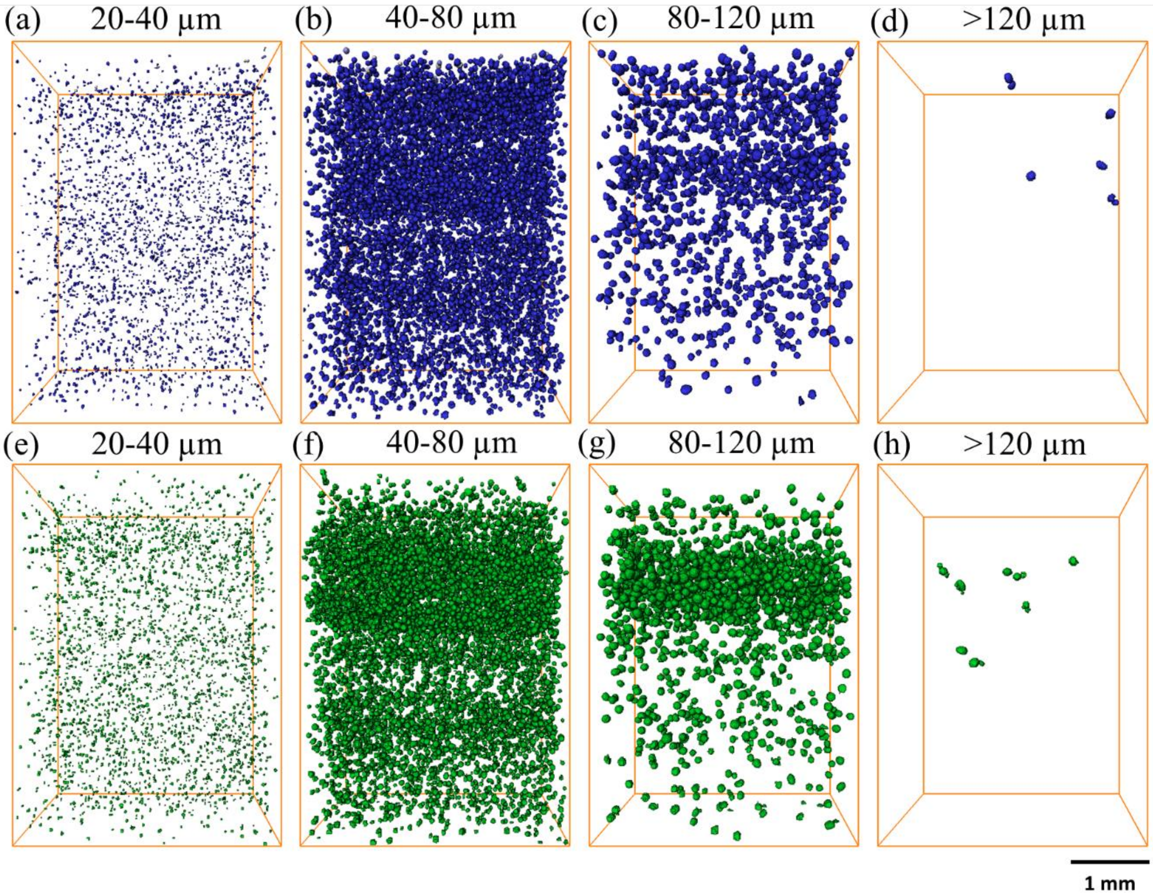

Fig. 9. 3D segregated visualization of the particles distribution in the samples for the groove filling method with 4 (a-d) and 8 (e-h) FSP passes, in function of the equivalent diameter (d_{eq}) range: 20 – 40 µm, 40 – 80 µm, 80 – 120 µm and above 120 µm.

3.5. Mechanical properties

In order to determine the effect of the pre-integration strategy on the mechanical properties, uniaxial tensile tests have been conducted on the composites manufactured after 8 FSP passes with both the multi-holes and groove strategies. Due to the fact that for the multi-holes condition 4 passes cannot fully homogenize the NiTi particles along the sample (Fig. 6a), only 8 FSP passes will be used for the comparison between the two studied filling conditions. A more homogeneous distribution is expected to result in higher material ductility, as lower strain localization is generated. Two tests have been performed for each condition and the results are highly reproducible. The representative engineering stress-strain curves are presented in Fig. 10.

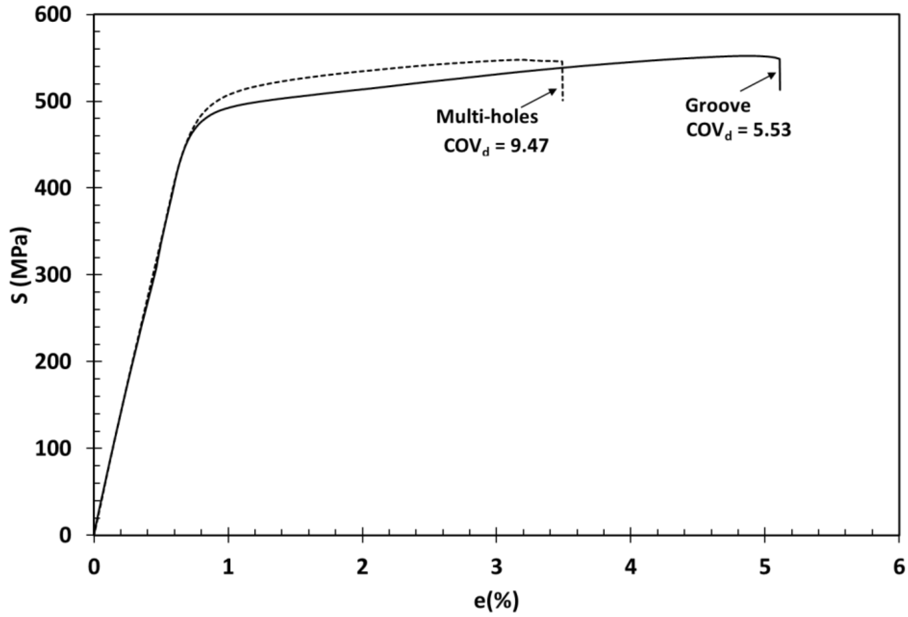

Fig. 10. Tensile curves of composites manufactured with 8 FSP passes using the multi-holes and the groove filling methods.

The mechanical strength is almost identical for the two strategies, while the groove filling method grants significantly higher ductility, though it involves almost 3 times the volume fraction of reinforcements compared to the multi-holes condition. According to (Deng and Chawla, 2006), an increase in particle clustering can result in slightly higher yield strength, while accompanied with a significant reduction in ductility. The authors showed that a lower COVd value was associated with higher ductility, owing to a more homogenous microstructure. In the present study, the groove filling strategy results in a significantly lower COVd value (reported under the curve in Fig. 10) and correspondingly a higher ductility compared to the multi-holes filling strategy. This is in agreement with what was concluded in the work of Deng and Chawla (2006). Song (2009) reported that the increase of V_f of SiC particles decreased the ductility of the SiC/Al composites. In the present work, however, the groove filling method leads to a higher V_f and still a higher elongation. This confirms that the homogeneity of the particle distribution is the main reason for the difference in elongation between the groove filling method and the multi-holes filling method, while the volume fraction of the reinforcements plays a secondary role.

It is thus reasonable to conclude that the higher ductility with the groove filling method can be attributed to the more homogeneous NiTi particle distribution in the aluminum matrix. Nevertheless, the identical mechanical strength for both conditions needs further investigation, given that this phenomenon is not in line with expectations for particle reinforced composites. Indeed, they are supposed to present higher strength with higher reinforcement content. This may be related to the precipitation kinetics of the Al base material around the NiTi particles, in particular in the precipitate free zones.

The present work opens up the pathway to the tailoring of mechanical properties of 7xxx series Al alloys through integration of reinforcements. This new manufacturing approach can be used as a starting point for future studies that, for example, aim to tune the damage mechanism or fracture propagation trajectory using the shape memory effect of the NiTi particles or the mechanical strength with other micronsized or nanosized reinforcements. The enhancement of fracture toughness has already been achieved in low strength Al1050 alloy by Zhao et al. (2019). Further investigations should also be oriented to improve the resistance to fatigue crack growth which is more relevant to industrial applications.

4. Conclusions

- A novel approach using mixed powder is proposed to manufacture NiTi particle reinforced Al7075 composites by friction stir processing (FSP). This new approach allows overcoming issues of particle clustering encountered when using solely reinforcement powder.
- Statistical analysis from HRXCT datasets shows that multiple passes can progressively homogenize the NiTi particle distribution in the aluminum matrix when using the multi-holes filling method. An increase in the nearest neighbor distance (NN_D) has been observed with more passes (8 passes vs. 4 passes), indicating a more homogeneous microstructure.
- For the groove filling method, no further improvement in the NiTi particle distribution can be observed after 4 passes, which means that the distribution homogenizes more quickly than in the case of multi-holes condition.
- The coefficient of variation of the mean nearest neighbor distance (COVd) is an efficient parameter to characterize spatial distribution homogeneity. Larger value of COVd is associated with higher level of inhomogeneity in the microstructure. In the present study, the groove filling method leads to lower value of COVd compared to the multi-holes filling method for the same number of FSP passes.
- Bimodal distributions have been observed for the equivalent diameter (d_{eq}) for all conditions. The groove condition prevails over the multi-holes condition in terms of impeding particle fragmentation.
- The particle distribution exhibits dependency on the particle size. Smaller particles are found to be homogeneously distributed throughout the sample while larger ones tend to agglomerate near the top of the sample.
- For the same number of FSP passes, the groove filling strategy yields higher ductility and similar strength compared to the multi-holes filling strategy. The higher ductility is expected to mainly originate from the more homogenous NiTi particle distribution in the aluminum matrix.

Declarations of interest

None.

Acknowledgments

This research work has been exclusively supported by the European Research Council (ERC) under the European Union’s Horizon 2020 research and innovation program (grant agreement n716678). The authors would like to thank Prof. Dr. Murat Tiryakioglu for his constructive comments.

References

Anderson, T.W., Darling, D.A., 1954. A Test of Goodness of Fit. Journal of the American Statistical Association 49, 765-769.

Buehler, W.J., Gilfrich, J.V., Wiley, R.C., 1963. Effect of Low - Temperature Phase Changes on the Mechanical Properties of Alloys near Composition TiNi. Journal of Applied Physics 34, 1475-1477.

Cai, W., Meng, X.L., Zhao, L.C., 2005. Recent development of TiNi-based shape memory alloys. Current Opinion in Solid State and Materials Science 9, 296-302.

Deng, X., Chawla, N., 2006. Modeling the effect of particle clustering on the mechanical behavior of SiC particle reinforced Al matrix composites. Journal of Materials Science 41, 5731-5734.

Dixit, M., Newkirk, J.W., Mishra, R.S., 2007. Properties of friction stir-processed Al 1100–NiTi composite. Scripta Materialia 56, 541-544.

Gangil, N., Maheshwari, S., Nasr, E., El-Tamimi, A., El-Meligy, M., Siddiquee, A., 2018. Another Approach to Characterize Particle Distribution during Surface Composite Fabrication Using Friction Stir Processing. Metals 8, 568.

Heinz, A., Haszler, A., Keidel, C., Moldenhauer, S., Benedictus, R., Miller, W.S., 2000. Recent development in aluminium alloys for aerospace applications. Materials Science and Engineering: A 280, 102-107.

Huang, G., Wu, J., Hou, W., Shen, Y., 2018. Microstructure, mechanical properties and strengthening mechanism of titanium particle reinforced aluminum matrix composites produced by submerged friction stir processing. Materials Science and Engineering: A 734, 353-363.

Huang, W., 2002. On the selection of shape memory alloys for actuators. Materials & Design 23, 11-19.

Lyman, T., 1964. Metals Handbook: Heat treating, cleaning and finishing. American Society for Metals.

Mishra, R.S., Ma, Z.Y., Charit, I., 2003. Friction stir processing: a novel technique for fabrication of surface composite. Materials Science and Engineering: A 341, 307-310.

Mishra, R.S., Mahoney, M.W., 2001. Friction Stir Processing: A New Grain Refinement Technique to Achieve High Strain Rate Superplasticity in Commercial Alloys. Materials Science Forum 357-359, 507-514.

Mishra, R.S., Mahoney, M.W., McFadden, S.X., Mara, N.A., Mukherjee, A.K., 1999. High strain rate superplasticity in a friction stir processed 7075 Al alloy. Scripta Materialia 42, 163-168.

Netto, N., Tiryakioğlu, M., Eason, P.D., 2018. On Si Redistribution During Friction Stir Processing of Cast Al-7%Si–0.4%Mg Alloys, In: Martin, O. (Ed.), Light Metals 2018. Springer International Publishing, Cham, pp. 417-422.

Ni, D.R., Ma, Z.Y., 2014. Shape Memory Alloy-Reinforced Metal-Matrix Composites: A Review. Acta Metallurgica Sinica (English Letters) 27, 739-761.

Ni, D.R., Wang, J.J., Zhou, Z.N., Ma, Z.Y., 2014. Fabrication and mechanical properties of bulk NiTip/Al composites prepared by friction stir processing. Journal of Alloys and Compounds 586, 368-374.

Otsu, N., 1979. A Threshold Selection Method from Gray-Level Histograms. IEEE Transactions on Systems, Man, and Cybernetics 9, 62-66.

Otsuka, K., Ren, X., 2005. Physical metallurgy of Ti–Ni-based shape memory alloys. Progress in Materials Science 50, 511-678.

Porter, G.A., Liaw, P.K., Tiegs, T.N., Wu, K.H., 2001. Fatigue and fracture behavior of nickel–titanium shape-memory alloy reinforced aluminum composites. Materials Science and Engineering: A 314, 186-193.

Prado, R.A., Murr, L.E., Soto, K.F., McClure, J.C., 2003. Self-optimization in tool wear for friction-stir welding of Al 6061+20% Al2O3 MMC. Materials Science and Engineering: A 349, 156-165.

Rana, H., Badheka, V., 2018. Influence of friction stir processing conditions on the manufacturing of Al-Mg-Zn-Cu alloy/boron carbide surface composite. Journal of Materials Processing Technology 255, 795-807.

Rana, H.G., Badheka, V.J., Kumar, A., 2016. Fabrication of Al7075 / B4C Surface Composite by Novel Friction Stir Processing (FSP) and Investigation on Wear Properties. Procedia Technology 23, 519-528.
Sharma, V., Prakash, U., Kumar, B.V.M., 2015. Surface composites by friction stir processing: A review. Journal of Materials Processing Technology 224, 117-134.
Song, M., 2009. Effects of volume fraction of SiC particles on mechanical properties of SiC/Al composites. Transactions of Nonferrous Metals Society of China 19, 1400-1404.
Thorat, R.R., Risanti, D.D., San Martín, D., Garces, G., Rivera Díaz del Castillo, P.E.J., van der Zwaag, S., 2009. On the transformation behaviour of NiTi particulate reinforced AA2124 composites. Journal of Alloys and Compounds 477, 307-315.
Tiryakioglu, M., Netto, N., 2018. Friction Stir Processing: Effect on Microstructure and Mechanical Properties in Cast Aluminum Alloys.
Weibull, W., 1939. The phenomenon of rupture in solids. Royal Swedish Institute for Engineering Research, Proc, p. 55.
Williams, J.C., Starke, E.A., 2003. Progress in structural materials for aerospace systems11The Golden Jubilee Issue—Selected topics in Materials Science and Engineering: Past, Present and Future, edited by S. Suresh. Acta Materialia 51, 5775-5799.
Yang, N., Boselli, J., Sinclair, I., 2001. Simulation and quantitative assessment of homogeneous and inhomogeneous particle distributions in particulate metal matrix composites. Journal of microscopy 201, 189-200.
Zeng, X.H., Xue, P., Wang, D., Ni, D.R., Xiao, B.L., Ma, Z.Y., 2018. Effect of Processing Parameters on Plastic Flow and Defect Formation in Friction-Stir-Welded Aluminum Alloy. Metallurgical and Materials Transactions A 49, 2673-2683.
Zhao, L., Ding, L., Soete, J., Idrissi, H., Kerckhofs, G., Simar, A., 2019. Fostering crack deviation via local internal stresses in Al/NiTi composites and its correlation with fracture toughness. Composites Part A: Applied Science and Manufacturing, 105617.